Indian J Phys
DOI 10.1007/s12648-013-0365-6

ORIGINAL PAPER

Optical properties of green synthesized ZnO nanocomposites

S Deb[1]*, P K Kalita[2] and P Datta[1]

[1]Department of Electronics Science and Communication Technology, Gauhati University, Guwahati 781014, Assam, India

[2]Department of Physics, Guwahati College, Guwahati 781021, Assam, India

Received: 29 April 2013 / Accepted: 12 July 2013

Abstract: A green synthesis route using starch as a capping agent was effectively employed to synthesize ZnO nanostructures through chemical bath deposition. Sodium borohydride was used in one of the approaches in synthesis. Broadening of X-ray diffraction peaks suggested formation of nanosize ZnO in agreement with the high resolution transmission electron microscopy images. As-synthesized ZnO nanostructures were polycrystalline having wurtzite type structure. Average size of the particles was about 8 nm which was in close agreement with measurements from optical studies. Starch was found to play a key role in bringing the strong quantum confinement in ZnO particles. Optical absorption edge was found to be around 240–275 nm which exhibited a clear large blue shift and thereby enhancement of band gap energy. A strong green photoluminescence emission at 604.5 nm was observed in ZnO nanoparticles synthesized using sodium borohydride and may be attributed to the defect controlled recombination mechanism.

Keywords: ZnO; HRTEM; PL; Green synthesis

PACS Nos.: 81.05.Gc; 81.16.Ta; 78.66.Jg

1. Introduction

The synthesis, characterization and processing of nanostructure materials are parts of an emerging and rapidly growing research work in recent times [1, 2]. Controlled microstructural characteristics in co-relation to optoelectronic properties are becoming important especially for the application point of view. Although elemental semiconductors have been very useful for development of microelectronics, they have some drawbacks. The fundamental band gap of these semiconductors is indirect, which implies that they emit very feeble light and their absorption coefficients are low. For optoelectronic applications, compound semiconductor materials offer many desired properties and could be synthesized with much ease [3]. ZnO is well-known as a direct band gap compound semiconductor with a wide band-gap of 3.37 eV room temperature and have distinguished performance in electronics, optics and photonics [4–6]. As it is rich in nature, chemically stable and environmentally friendly, it is expected to obtain devices with a major improvement in cost/performance ratio. Again, its high exciton binding energy (60 meV) can ensure efficient excitonic emission even at room temperature [7], implying high radiative recombination effectiveness for spontaneous emission plus a lower threshold voltage in favour of laser emission. Thus, studies have been carried to tailor the properties [8, 9] of ZnO effectively to adopt it for varied applications. However, it has been observed that a great number of surface atoms produce high surface energy nanoparticles, which make them very reactive. Thus systems without protection of their surfaces can have aggregation as reported by Wei et al. [10]. In this context, passivator plays a great role. As other organic passivator may result in environmental pollution on large-scale production, starch also termed as "green" passivator is selected for being environmentally friendly and non-toxic [11, 12]. Besides, it is also reported that the starch is considered as a good polymer to cap nano-sized materials as it has the polar groups in its structures, such as SO_3^2 and OH^2 which perform as synchronic sites for ion aggregation between particles [13]. Several authors [14–16] have reported the use of various deposition techniques to synthesis ZnO nanostructures.

Starch is the reserve substance in plant cells, a polymer of D-glucopyranose units linked by a-1,4 glycosidic linkages

*Corresponding author, E-mail: sujatabmk@gmail.com

Published online: 25 July 2013

[17]. In addition, these polysaccharides are preferred over others as it is renewable and a good diffusion approach to form stable ZnO. It has also been reported that hydroxyl groups of polysaccharides work to obtain uniform structures as well as to protect semiconductor nanoparticles from aggregation [18]. In this paper, we present synthesis of ZnO nanoparticles through green synthesis route, using starch as capping agent and sodium hydroxide as well as sodium borohydride as precursors. The structural and optical properties have been studied and co-related with growth conditions.

2. Experimental details

All chemicals were of analytical research grade (Merck) and used in the experiments as received with no further refinement. ZnO nanoparticles were prepared by chemical bath deposition method using zinc acetate and choosing precursors, sodium hydroxide and sodium borohydride alternately and soluble starch as a capping agent in both the approaches. A soluble starch (3 %) stock solution was prepared in distilled water under constant stirring at 60 °C for about 6 h for complete solubilization. A 0.5 M solution of zinc acetate i.e., $Zn(CH_3COO)_2 \square 2H_2O$ was prepared and mixed with the starch solution under constant stirring for good dispersion. In this starch capped zinc acetate solution, sodium hydroxide (NaOH) solution was mixed drop wise with constant stirring and the resulting solution was heated at 80 °C about one and half hour. A milky white colour of the resulting reaction mixture indicated formation of ZnO nanostructures (sample I). In another approach, solution of sodium borohydride i.e., $NaBH_4$ was prepared and added drop wise to the starch capped zinc acetate solution. A white complex was formed, which was due to reduction of zinc ions. After stabilization the mixture was subjected to prolonged heating at 80 °C for formation of ZnO under normal oxidation in air (sample II). Cleaned glass slides were dipped in the resultant matrix solutions to obtain thin films for XRD studies. Colloidal solutions were taken for an optical as well as HRTEM studies. The samples were stored in air tight desiccators at room temperature for characteristic studies.

X-ray diffractometrogram for the synthesized materials was studied in a Philips diffractometer (model-XPERT-PRO), over an angular range of 10°\ 2h\ 75° in continuous scan mode with step scan 0.05 using Cu-Ka radiation (k = 1.5406 Å). Structural characterizations were recorded on a high resolution transmission electron microscope (JEOL JEM-2100) operated at voltage 200 kV. Selected area electron diffraction (SAED) patterns were also taken along with prominently observed d-values in HRTEM measurements. Photoluminescence spectrum of the ZnO nanoparticles was recorded using a Hitachi FL spectrophotometer (model-F-2500), with excitation wavelength of 300 nm. Optical absorption spectra were recorded using a Shimadzu UV–visible spectrophotometer (model-UV-1800), in the range 200–800 nm.

3. Results and discussion

Figure 1 shows X-ray diffraction (XRD) pattern of as-prepared ZnO nanostructures (sample I). It shows that the film is polycrystalline having diffraction peaks corresponding to (100), (002), (101) and (110) planes that indicate typical hexagonal wurzite type structure of ZnO quantum dots. Observed diffraction planes are in good agreement with JCPDS file no. 36-1451. No diffraction peaks of Zn or other impurities are observed in as-prepared sample, which confirms homogeneous synthesis of ZnO using NaOH. However, as-prepared sample shows diffraction peaks at 33.27° (211) and 59.48° (511) that can be indexed to orthorhombic form of $Zn(OH)_2$. This is in good agreement with JCPDS card No. 38-0385 and is supported by earlier reports [19, 20]. Possibility of existence of $Zn(OH)_2$ is explained by different workers under varied reaction conditions, depending on parameters, such as synthesis temperature and pH value [21, 22]. Nicholas et al. [21] have proposed that below 60 °C, $Zn(OH)_2$ is the key product and ZnO is expected to form with increase in synthesis temperature. Some authors [22] have reported methods to control shape of ZnO particles at various pH values and demonstrate how to stabilize $Zn(OH)_2$. A few other workers [20, 23] have investigated on conversion of e-$Zn(OH)_2$ to ZnO and have discussed detailed mechanism involved. In this study, $Zn(OH)_2$ is confirmed from diffraction peak positions that are supported by JCPDS card No. 38-0385 and presence of this zinc hydroxide species is most probable due to surface hydroxylation of ZnO.

Lattice parameters of hexagonal wurtzite ZnO are calculated from most prominent peaks using the following relation,

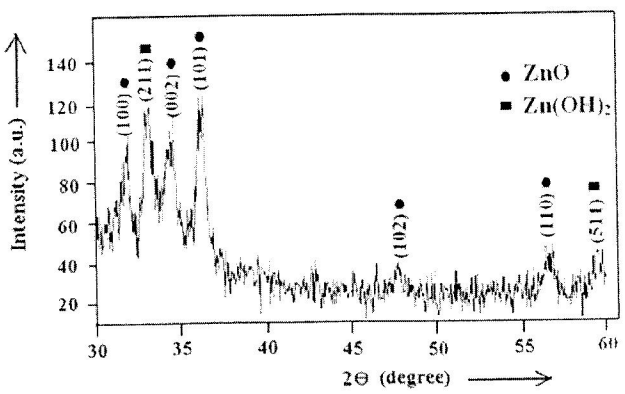

Fig. 1 XRD pattern of starch capped ZnO nanoparticles (sample I)

$$\frac{1}{d^2} = \frac{4}{3}\left[\frac{h^2 + hk + k^2}{a^2}\right] + \frac{l^2}{c^2} \quad (1)$$

which gives lattice constant a = 3. 249 Å and c = 5.207 Å that are in good agreement with standard JCPDS data. XRD results are in close agreement with previous report [24]. The most preferred orientation is expected along (101) direction. Average particle size D has been estimated by using Debye–Scherrer formula,

$$D = \frac{0.9\lambda}{b\cos\theta} \quad (2)$$

where k is wave length of X-ray (0.1541 nm), b is FWHM (full width at half maximum) and h is diffraction angle [25]. The calculated particle size is nearly 8 nm which is in fair agreement with size estimated from optical studies.

Figure 2(a) and 2(b) show HRTEM images of the samples respectively. HRTEM image of sample I shows well-defined particle distribution having average particle size 8 nm. HRTEM image shows that ZnO nanoparticles are nearly spherical in shape and well dispersed in starch. SAED of ZnO shown in Fig. 2(c) displays a set of uniform bright diffraction rings corresponding to hexagonal wurtzite structure. Diffraction rings of ZnO nanoparticles suggest that the nanoparticles have mostly preferential orientation instead of random orientation. HRTEM image in Fig. 2(d) shows particles having spacing of * 0.26 nm, which matches very well with (002) lattice plane of wurtzite phase of ZnO.

UV–visible spectra of the samples I and II are shown in Fig. 3(a) and 3(b) respectively. Absorption edge is found to be around 275 nm for sample I as depicted in Fig. 3(a) while Fig. 3(b) shows a prominent excitonic absorption peak at around 240 nm and a few small humps at around 345 and 380 nm for sample II. Excitonic absorption lies much below the band gap wavelength of bulk ZnO (365 nm) [26], illustrating that nanocomposite exhibits a blue-shift compared to that of bulk ZnO, due to quantum confinement effect. Again, absorption of ZnO is very sharp indicating monodispersed nature of ZnO nanoparticle distribution, as reported by other workers [27, 28]. Polysaccharides in starch have a dominant diffusion approach to form stable ZnO. Also hydroxyl groups of polysaccharides work to obtain uniform structures as well as protect ZnO nanoparticles from aggregation [18]. Additional small peaks are attributed to surface states mainly arising from dangling bonds. It is observed that the blue shifts are quite large indicating a strong quantum confinement of exciton. The electron and hole wave functions of exciton therefore overlap and as a result, respective bands become discrete energy states and raise the forbidden band gap energy. Enhancement of band gap energy (DE) over bulk is inversely proportional to square of radius (R) of nanoparticle and that can be approximately related as

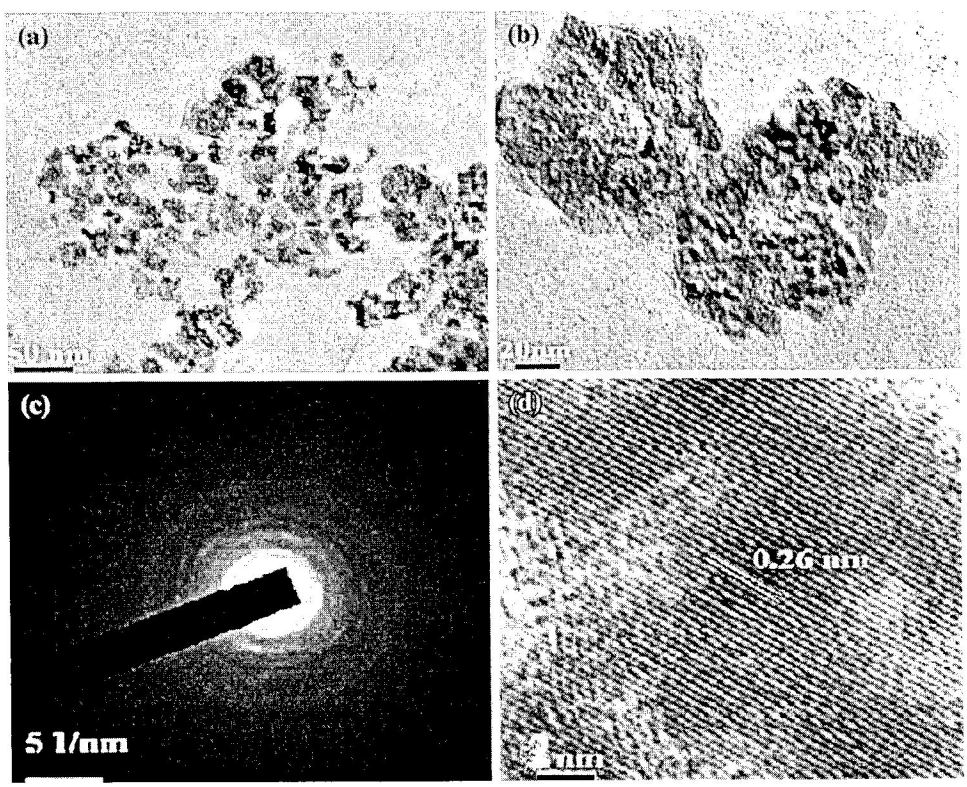

Fig. 2 HRTEM images of ZnO at a resolution of (a) 50 nm, (b) 20 nm, corresponding, (c) SAED pattern and (d) observed d-values

$$\Delta E = \hbar^2 p^2 = 2\mu R^2 \qquad (3)$$

Here μ is reduced mass of effective electron and hole mass of exciton in ZnO nanoparticles. Considering parabolic band structure of ZnO nanoparticles, above effective mass approximation (EMA) method was used for estimation of particle size (2R) which is found to be 4.5–6 nm.

Pl spectrum of ZnO nanostructure of sample I has been depicted in Fig. 4(a). It shows near band gap emission at 380 nm and another extrinsic emission at 480 nm from inherent defects produced in sample. Observed near band gap photoluminescence is result of radiative recombination of electrons and holes confined in nanoparticles, whereas extrinsic emission is governed by surface defects. Surface of a nanoparticle is very sensitive and reactive. There are lots of unsaturated bonds on the surface of ZnO forming gap surface states. A part of the electrons excited to conduction band would first transfer to surface states lying in mid band gap and then recombine nonradiatively with holes in valence band, correspondingly reducing the emission intensity.

It is noted that a strong maximum of 604.5 nm green wavelength as appeared in PL spectrum of sample II as shown in Fig. 4(b). It is known that visible and infrared emissions initiate from oxygen and zinc interstitials and vacancies [29]. Oxygen vacancies often are able to work as luminescence centers. In present work, emission peak around 604.5 nm can be assigned to originate from defect state luminescence. Moreover, sodium borohydride, one of the precursors is a reducing agent, which reduces metal ion thus residual zinc particles is formed first which are then oxidized to form ZnO on heating. However oxidation is expected to be partial at 80 °C so that ZnO shell is formed over Zn particles and thereby forming Zn/ZnO core/shell type nanostructures. Zn core and sheathing ZnO shell have a large lattice mismatch in their epitaxial relationship. Thus, the interface between them plays a key role in determination of optoelectronic properties that has also been reported by Ding et al. [30]. Moreover, Zhang et al. [29] have investigated structure and photoluminescence of Zn/ZnO core–shell nanostructure at different heating temperatures and have proposed that width of depletion layer directly affects intensity of green emission. Thinner the depletion layer,

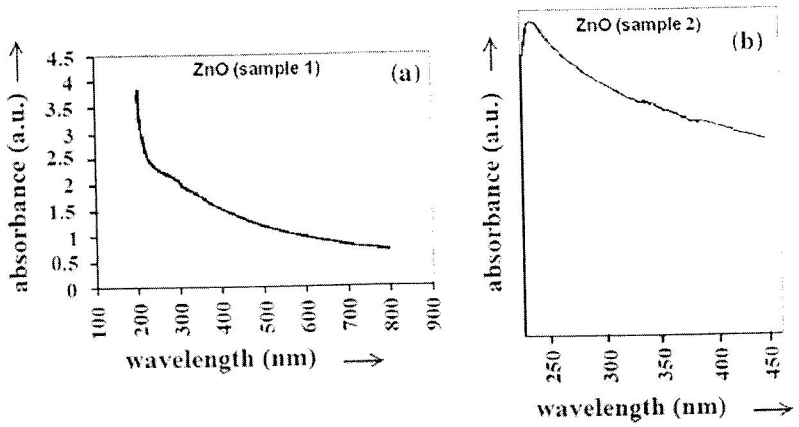

Fig. 3 UV Spectra of ZnO nanoparticles (a) sample I (b) sample II

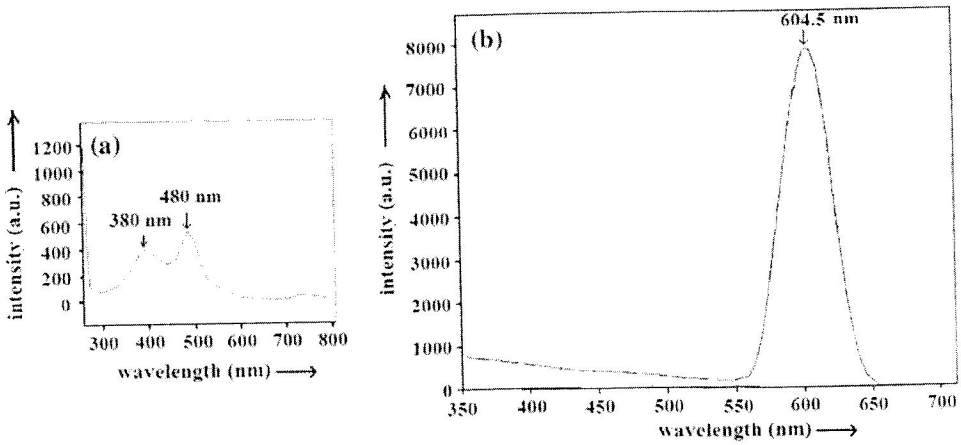

Fig. 4 PL emission spectra of ZnO nanoparticles: (a) sample I and (b) sample II

Table 1 Absorption and emission characteristics of sample I and sample II showing absorption edge (k_a), near band gap emission (k_e), impurity emission (k_i), band gap (E_g) and particle size (D)

Sample	k_a (nm)	k_e (nm)	k_i (nm)	E_g (eV)	D (nm)
1	275	380	480	4.5	4.5
2	240	–	604.5	5.16	6

stronger is the green emission intensity. Therefore, a direct relationship between temperature and PL study of Zn has been established. Our finding of a strong green emission intensity that appears in PL spectrum of sample II with a partial increase in temperature supports Ding et al.'s [30] proposition. Core–shell Zn/ZnO structure can thus be well thought-out as a Schottky barrier. In present case, green luminescence mainly originates from defect states such as singly ionized oxygen vacancies are left over zinc oxide. It has been found heating has a great effect in that apart from Zn oxidation, Zn core is further oxidized at core–shell interface by diffused oxygen from outer surface to shell. Luminescence peak is strong having higher intensity and symmetry, which suggests formation of well-defined uniform distribution of Zn/ZnO nanocomposites. Thus, green emission results from the recombination of a photo generated holes with singly ionized oxygen vacancies.

The absorption and emission characteristics of sample I and sample II ZnO nanostructures have been summarized in Table 1.

4. Conclusions

ZnO is synthesized by a simple chemical bath deposition method using starch as capping agent. XRD shows presence of hexagonal wurtzite type ZnO nanostructure which is also confirmed by EDS pattern of HRTEM images. HRTEM morphology shows formation of spherical shaped ZnO nanostructures with average size 8 nm. UV–visible spectra show the prominent excitonic absorption peak at around 240–275 nm for both samples synthesized with and without sodium borohydride, which exhibits a clear large blue-shift compared to that of bulk ZnO. This can be attributed to strong quantum confinement effect governed by hydroxyl groups of polysaccharides present in starch. Photoluminescence (PL) spectra show sharp distinction between both samples. It shows a near band gap emission at 380 nm and a long wavelength emission at 480 nm for ZnO (sample I) synthesized using usual NaOH. Here green emission results from recombination of a photo generated hole with a singly ionized charge state of native defects. On the other hand, a strong green photoluminescence emission at 604.5 nm is observed for ZnO nanoparticles while using sodium borohydride as precursors. This suggests formation of Zn/ZnO core/shell type nanocomposites with a high density of oxygen vacancies. Thus, visible green luminescence can be tuned using sodium borohydride in synthesis process which may open up paths to much technological application in visible light emitting and nanophotonic devices at low cost.

Acknowledgments We thank Department of Chemistry G.U., IIT, Guwahati and SAIF, Shillong for technical supports.

References

[1] S Mitra, A Mandal, S Banerjee, A Dutta, S Bhattacharya, A Bose and D Chakravorty Indian J. Phys. 85 649 (2011)
[2] S Bhattacharya and A Ghosh Appl. Phys. Lett. 88 133122 (2006)
[3] S Mondal and P Mitra Indian J. Phys. 87 125 (2013)
[4] C A Mirkin Science 286 2095 (1999)
[5] R Chakraborty, U Das, D Mohanta and A Choudhury Indian J. Phys. 83 553 (2009)
[6] M C Newton and R Shaikhaidarov Appl. Phys. Lett. 94 153112 (2009)
[7] U Ougur, Y I Alivov, C Liu, A Teke, M A Reshchikov, S Dogan, V Avrutin, S J Cho and H Morkoc J. Appl. Phys. 98 041301 (2005)
[8] M L Dinesha, G D Prasanna, C S Naveen and H S Jayanna Indian J. Phys. 87 147 (2013)
[9] S Bhattacharya and A Ghosh J. Nanosci. Nanotechnol. 7 3684 (2007)
[10] Q Wei, S-Z Kang and J Mu Colloids Surf. A: Physicochem. Eng. Aspects 247 125 (2004)
[11] P Rodrıguez, N Munoz-Aguirre, E San-Martin Martınez, G Gonzalez, O Zelaya and J Mendoza Appl. Surf. Sci. 255 740 (2008)
[12] K Senthilkumar, T Kalaivani, S Kanagesan and V Balasubramanin J. Appl. Phys. 112 114331 (2012)
[13] D J Thomas and W A Atwell Starches (St. Paul, MN, United States: Eagan Press) p 8 (1999)
[14] D Polsongkram, P Chamninok, S Pukird, L Chow, O Lupan, G Chai, H Khallaf, S Park and A Schulte Phys. B 403 3713 (2008)
[15] O Lupan, L Chow, S Shishiyanu, E Monaico, T Shishiyanu, V Sontea, B R Cuenya, A Naitabdi, S Park and A Schulte Mater. Res. Bull. 44 63 (2009)
[16] P Mitra and S Mondal Prog. Theor. Appl. Phys. 1 17 (2013)
[17] A L M D Leitao Mycofactories (Portugal: Bentham Science) p 4 (2011)
[18] P Rodriquez, N Munoz-Aguirre, E San-Martin Martinez, G Gonzalez de la Cruz, S A Tomas and O Zelaya-Angel J. Cryst. Growth 310 160 (2008)
[19] R A McBride, J M Kelly and D E McCormack J. Mater. Chem. 13 1196 (2003)
[20] G Mu PhD Thesis (Missouri University of Science and Technology, China) (2010)
[21] N J Nicholas PhD Thesis (University of Melbourne Victoria, Australia) (2011)
[22] P Amornpitoksuk and S Suwanboon Power Technol. 203 243 (2010)
[23] D Pradhan and K T Leung Langmuir 24 9707 (2008)
[24] A Jegan, A Ramasubbu, K Karunakaran and S Vasanthkumar Int. J. Nano Dimens. 2 171 (2012)
[25] N C Das, Upeti and P E Soko J. Exp. Nanosci. 5 180 (2010)
[26] C Jagadish and S J Pearton Zinc Oxide Bulk, Thin Films and Nanostructures: Processing, Properties and Applications (UK: Elsevier's Science and Technology) p 6 (2006)

[27] P Kumbhakar, D Singh, C S Tiwary and A K Mitra Chalcogen. Lett. 5 387 (2008)
[28] S C Singh, R K Swarnkar and R Gopal Bull. Mater. Sci. 33 21 (2010)
[29] X Y Zhang, J Y Dai, C H Lam, H T Wang, P A Webley, Q Li and H C Ong Acta Mater. 55 5039 (2007)
[30] Y Ding, X Y Kong and Z L Wang J. Appl. Phys. 95 306 (2004)